Proc. Natl. Acad. Sci. USA
Vol. 79, pp. 4967–4971, August 1982
Biophysics

Conformational substates in a protein: Structure and dynamics of metmyoglobin at 80 K

(low-temperature crystallography/Mössbauer absorption/Debye–Waller factor/intramolecular motion/lattice disorder)

H. HARTMANN*, F. PARAK*§, W. STEIGEMANN*, G. A. PETSKO†, D. RINGE PONZI†, AND H. FRAUENFELDER‡

*Max-Planck Institut für Biochemie, 8033 Martinsried, Federal Republic of Germany; †Department of Chemistry, Massachusetts Institute of Technology, Cambridge, Massachusetts 02139; and ‡Department of Physics, University of Illinois at Urbana-Champaign, Urbana, Illinois 61801

Communicated by R. L. Mössbauer, May 14, 1982

ABSTRACT **The crystal structure of sperm whale metmyoglobin has been determined at 80 K to a resolution of 2 Å. The overall structure at 80 K is similar to that at 300 K except that the volume is smaller. Refinement of the structure by the method of restrained least squares (current $R = 0.175$) permits the assignment of isotropic atomic mean-square displacements to all nonhydrogen atoms. Comparison with the values obtained earlier at 250–300 K indicates that the protein at 80 K is more rigid. The average experimentally determined Debye–Waller factor, B, for the protein is 14 Å^2 at 300 K and 5 Å^2 at 80 K. Plots of backbone mean-square displacement vs. temperature show a discontinuity of slope for at least one-third of all residues. This behavior is in good agreement with the temperature dependence of the mean-square displacement of the heme iron as measured by Mössbauer absorption. The magnitudes of the smallest mean-square displacements observed at 80 K indicate that intramolecular motions can be frozen out to a surprisingly large degree. Even at 80 K, however, some atoms in myoglobin still have mean-square displacements greater than 0.1 Å^2, thus providing evidence for conformational substates.**

The view of protein molecules as systems that fluctuate over a large number of conformational substates is now accepted (1–3). Conformational fluctuations are important for biological function, and detailed studies of their properties are therefore desirable. Myoglobin (Mb), "the hydrogen atom of biology," is a good choice for such studies. Mb is presumed to have a simple function, storage and transport of oxygen in muscles (4). Some of its properties can be understood in terms of its static three-dimensional structure, determined by single-crystal x-ray diffraction at 300 K (5, 6). However, dynamic features, especially the access of oxygen to the heme and the kinetics of binding of carbon monoxide to the iron (7, 8), cannot be explained by a static picture. X-ray crystallography is a powerful tool for mapping average displacements of atoms in a protein (9–11). Here, we present the determination of the structure of metMb at 80 K to a resolution of 2 Å and compare this structure and atomic displacements with earlier results at 250–300 K and with the results of Mössbauer absorption studies at 4.2–300 K (12–14).

Atomic displacements are involved in the interconversion of different local configurations (conformational substates) of the same overall protein structure (7–14). Different conformational substates perform the same biological function, albeit possibly with different rates. Transitions from one substate to another require the surmounting of potential energy barriers. If the barriers are very large compared with k_BT, the distribution of substates is static. If the barriers are small, the distribution is dynamic and a molecule can move from one substate to another, even at low temperatures. The idea that a dynamic distribution can still exist at low temperatures is at first surprising. However, consider for simplicity an atom that can occupy either of two positions separated by a barrier of height H_0. The time τ_R characteristic for transitions between the two positions then is given approximately by $\tau_R = \tau_0 \exp(H_0/RT)$, with $\tau_0 \simeq 10^{-13}$ s. Fluorescence quenching (15) and Rayleigh scattering (16) imply barrier heights of about 25 kJ/mol. At 80 K, $H_0 = 25$ kJ/mol gives $\tau_R \simeq 10^3$ s. During typical x-ray experiments, which last about 10^5 s, conformational substates can equilibrate even at 80 K. If, moreover, the bottoms of the two conformational positions differ by 1 kJ/mol or less, both substates will be appreciably populated even at 80 K.

Information about the spatial distribution of conformational substates can be expressed in terms of individual atomic mean-square displacements, $\langle x^2 \rangle$. By measuring these atomic displacements as a function of temperature, the shape of the effective conformational potential well in which the atom moves can be determined. In earlier crystallographic work, mean-square displacements have been measured at 220–300 K (9). The example given above shows that this temperature range is too small to explore the conformational potential. We have therefore extended the experiments to much lower temperatures. The technique described here indeed shows major changes in mean-square displacements in going from 300 to 80 K and opens up the possibility of answering a number of questions about the structure and dynamics of proteins. Similar work at low temperatures has been carried out with trypsin by Huber and co-workers (17), who reach analogous conclusions.

EXPERIMENTAL

Sample Preparation and Data Collection. Crystals of sperm whale metMb were grown from 3.75 M ammonium sulfate (pH 6.9), according to the published method (18). The crystals have the symmetry of space group $P2_1$, with one molecule of molecular weight 17,816 per asymmetric unit. Protein crystals are usually destroyed if they are cooled below the liquid–ice phase transition of the free mother liquor. There are, however, several methods to overcome this difficulty. Crystal shattering can be hindered by freezing under high pressure (19), exchanging the mother liquor of the protein crystal with a cryoprotectant (20), or shock freezing crystals containing their normal mother liquor (21). The last method has clear advantages: the solvent around the molecule is not modified and no physical changes should be introduced, in contrast to the application of high pres-

The publication costs of this article were defrayed in part by page charge payment. This article must therefore be hereby marked "*advertisement*" in accordance with 18 U. S. C. §1734 solely to indicate this fact.

§ To whom reprint requests should be addressed.

sure. A Mb crystal ($0.3 \times 0.4 \times 0.7$ mm^3) was shock frozen by plunging it into liquid propane and stored in liquid nitrogen. Diffraction experiments were carried out at 80 ± 2 K in a cryostat mounted on a Siemens two-arc diffractometer. The cryostat axis was coincident with the rotation axis. CuKα radiation filtered by a graphite monochromator completely bathed the crystal. Intensity data were measured photographically by using the screenless oscillation method on a cylindrical film cassette having a radius of 8.9 cm. The crystal oscillated around the b axis with an oscillation angle, $\Delta\phi$, of 6°. After each exposure of about 12 hr, the angle ϕ was increased by 5°. The total measurement covered the range $0° < \phi < 180°$. The shape of the film together with the window of the cryostat limits the maximum resolution to 2 Å perpendicular and 2.6 Å parallel to the oscillation axis, respectively. Films were evaluated by standard methods (22). Only fully recorded reflections were taken into account. Three films were used in a pack. A weighted film-to-film scaling was carried out. Photographs for different ϕ values were scaled together by using the reflections of the overlap region as well as symmetry equivalent reflections applying a linear scale factor only. We obtain a typical R_{sym} value of 0.07. From 17,965 observations, 4,589 unique reflections were obtained above a 2.0σ significance level with an R_{merge} value of 0.104. This number of reflections corresponds to about 55% of the total possible reflections at 2 Å resolution. The unobserved data are distributed roughly equally over the whole resolution range, but their effect on the absolute Debye–Waller B values determined by refinement is not known.

The unobserved data were due to the physical restrictions of the cryostat used and are not the weakest reflections. To assess the effect of 2 Å resolution on the overall and individual B values, we refined our 300 K Mb data at 2 Å resolution and compared the B values found with those obtained earlier using 1.5 Å data (9). There was no significant difference. We therefore believe these results with 2 Å data at 80 K to be accurate.

Crystallographic Refinement. The observed structure amplitudes, F_{obs}, were placed on an approximate absolute scale by comparison with the room temperature data of Watson (5). Calculated amplitudes, F_{calc}, and phase angles were computed for each reflection by using the atomic coordinates for sperm whale metMb at room temperature as refined by Takano (6). As a check on the quality of the measured data, the heme group and several amino acid side chains in the ligand binding pocket [histidine-64(E7), phenylalanine-43(CD1), and valine-68(E11)] and the side chain of the proximal histidine, histidine-93(F8), were omitted from the calculation. An electron density map was computed with coefficients $2F_{obs} - F_{calc}$ and calculated phase angles. Such a map is equivalent to the observed structure plus the difference between the observed and the calculated structures. This map clearly showed the familiar Mb molecule plus the omitted heme group and neighboring side chains. These residues were rebuilt into the structure by using a Vector General 3404 interactive computer graphics system with the fitting program FRODO (23). The resulting coordinate set served as the starting point for crystallographic refinement of the 80 K structure. Refinement, carried out by the restrained least-squares method of Konnert and Hendrickson (24), was begun by using an overall Debye–Waller factor and 2.5 Å data. Once the refinement progressed to include the high-resolution (2 Å) data, it was possible to refine individual isotropic Debye–Waller factors for each of the 1,261 nonhydrogen atoms in the protein, provided the restraints were kept tight. Covalent bond distances have been restrained to a current root-mean-square deviation of 0.03 Å from ideality, and bond angles have been restrained to a root-mean-square deviation of 12°. Up to now, 37 cycles of refinement have been performed. Bound solvent molecules have yet to be located, but further work is unlikely to change the parameters for the main chain and interior side chain atoms significantly. The current crystallographic R factor, defined as $R = \Sigma|F_{obs} - F_{calc}|/\Sigma F_{obs}$, the sums being taken over all reflections, is 0.175.

RESULTS AND DISCUSSION

The Shock-Freezing Technique. The smoothness of the refinement of the 80 K structure and the similarity of its atomic coordinates to those obtained from higher resolution data at 300 K show that it is possible to collect good data below the freezing point of the mother liquor without cryoprotectants. Our technique may prevent radiation damage in extremely radiation-sensitive protein crystals. It also forms the experimental basis for the direct-phase determination of x-ray reflections by Mössbauer scattering techniques (21, 25), which require temperatures of the order of 80 K.

Crystal Parameters. The shock-freezing technique does not change the space group of Mb crystals, but the unit cell dimensions at 80 K are considerably smaller than those at 300 K. At 80 K, $a = 63.44$ Å, $b = 30.45$ Å, $c = 34.05$ Å, $\beta = 105.6°$; at 300 K, $a = 64.56$ Å, $b = 30.97$ Å, $c = 34.86$ Å, $\beta = 105.86°$. The unit cell volume of 63,350 Å^3 is 4.5% smaller than at 300 K. There is no significant change in angular spread and no phase transition occurs on going to 80 K.

Overall Structure and Protein Volume. The overall structure of the protein at 80 K is very similar to that at 300 K, but the volume is smaller. At present, no computer program exists to calculate volumes for proteins at 80 K with appropriate corrections for the effect of very low temperature (26), so we have not attempted this calculation. However, the unit cell volume at 80 K is smaller than at 300 K, and measurements of interatomic distances between widely separated regions of the protein indicate that the helices are significantly shorter at 80 K.

Overall Debye–Waller Factor. Atomic and molecular motions, combined with crystal imperfections, cause the average reflection intensity to decrease with increasing scattering angle θ by the Debye–Waller (temperature) factor $\exp(-2B \sin^2\theta/\lambda^2)$, where λ is the wavelength of the incident radiation and B is related to $\langle x^2 \rangle$ by $B = 8\pi^2\langle x^2 \rangle$.

The overall B value for metMb at 300 K is 14 Å^2, which implies that $\langle x^2 \rangle = 0.175$ Å^2. The value of B for the 80 K structure is 5 Å^2, giving an $\langle x^2 \rangle$ of 0.063 Å^2. These overall fitted B values can be compared with the corresponding averages of the individual atomic B values, 6.5 Å^2 at 80 K and 12.2 Å^2 at 300 K. The least-squares refinement can fit an individual B_i to every atom, but the interpretation of this number in terms of atomic motion requires caution. Both the overall $\langle x^2 \rangle$ and the individual $\langle x^2_i \rangle$ values are sums of two quantities: $\langle x^2 \rangle = \langle x^2 \rangle_{cv} + \langle x^2 \rangle_{ld}$, where $\langle x^2 \rangle_{cv}$ is the displacement due to vibrational motion and substates and $\langle x^2 \rangle_{ld}$ is the contribution from disorder in the crystal lattice (9). Although the distinction between dynamic and static disorder was discussed in 1971 (27), many protein crystallographers believed until recently that lattice disorder dominated the overall $\langle x^2 \rangle$. The dramatic reduction in the overall $\langle x^2 \rangle$ of crystalline Mb on going from 300 to 80 K shows that, for this protein at least, actual motion and not lattice disorder is the major contributor to the apparent mean-square displacement. The observation of nonzero $\langle x^2 \rangle$ values on extrapolation of our data to $T = 0$ (see below) confirms that, for many atoms in the Mb crystal, the dominant contribution comes not from simple harmonic thermal vibration but from conformational substates (9). Even in the crystalline state, proteins are flexible.

Lattice Disorder. We have estimated the overall value of the lattice disorder $\langle x^2 \rangle_{ld}$ for Mb by comparing the $\langle x^2 \rangle$ values ob-

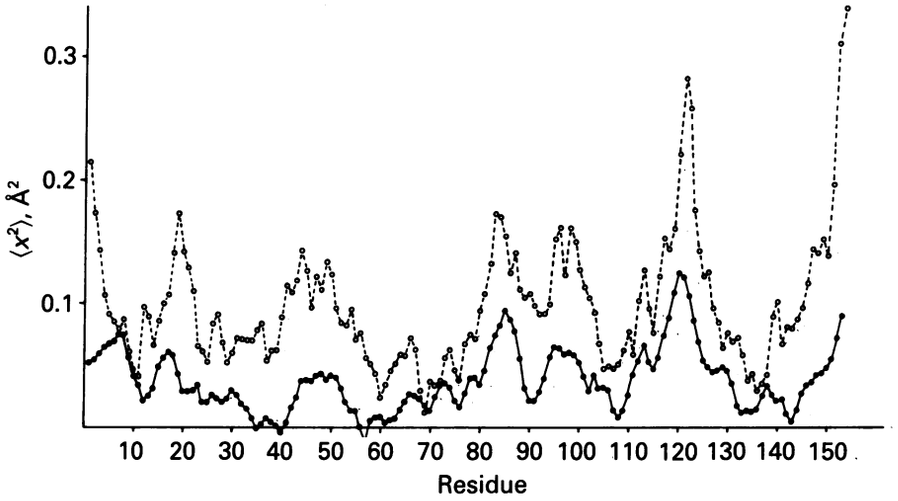

FIG. 1. Average backbone $\langle x^2 \rangle$ values for myoglobin vs. residue number. ●, 80 K; ○, 300 K. The average is taken over the N, C_α, and carbonyl C atoms only, since the $\langle x^2 \rangle$ values of the carbonyl O atoms are usually higher. An $\langle x^2 \rangle_{ld}$ of 0.045 Å^2 has been subtracted from the individual observed $\langle x_i^2 \rangle$ values.

tained for the iron atom by x-ray diffraction (9) and by Mössbauer absorption (13) at 250–300 K. Subtracting the resulting $\langle x^2 \rangle_{ld}$ = 0.045 Å^2 from the individual atomic $\langle x^2 \rangle$ obtained at 80 K leads to a number of values that are smaller than 0.01 Å^2, which is of the order of the zero-point vibrational $\langle x^2 \rangle$ observed for small-molecule crystals at low temperatures (28). Assuming that the freezing method did not *de*crease the lattice order (and the results certainly show that it did not *in*crease the disorder), the $\langle x^2 \rangle_{ld}$ value derived earlier (9) appears to be too large (see below). It should be emphasized that the limits of error of the $\langle x^2 \rangle$ values obtained from the x-ray analysis, estimated to be 0.018 Å^2 (9), are at least as large as the zero-point vibration $\langle x^2 \rangle$. In addition, any motion having a characteristic time slower than 0.1 μs does not contribute to the $\langle x^2 \rangle$ determined by the Mössbauer method. Therefore, if motions on this time scale contribute to the overall $\langle x^2 \rangle$ (and there is ample evidence that they must; K. Gersonde and G. N. La Mar, personal communication), the Mössbauer value underestimates the dynamic contribution and leads to overestimation of the lattice disorder term. Our refinement of the 80 K structure suggests that the correct value is closer to 0.025 Å^2. To facilitate comparison with earlier work, the value $\langle x^2 \rangle_{ld}$ = 0.045 Å^2 has been applied to the data in this paper. Whatever value is used for $\langle x^2 \rangle_{ld}$, the results show that lattice disorder does not dominate the overall or individual atomic displacements.

Individual Atomic Displacements. A graph of the average $\langle x^2 \rangle$ values of the backbone N, C_α, and carbonyl C atoms vs. residue number at 80 and 300 K is shown in Fig. 1. The main-chain displacements at 80 K do not exceed the corresponding values at 300 K. The shapes of the two curves agree well. The temperature dependence of the average $\langle x^2 \rangle$ values of backbone atoms of selected amino acids is shown in Fig. 2. The temperature dependences of the $\langle x^2 \rangle$ values for the iron atom, the atoms in the heme plane, and the proximal and distal histidines are compared with those from Mössbauer experiments on the iron in Fig. 3.

Comparison of the $\langle x^2 \rangle$ values at the four temperatures allows a discussion of some general features of the dynamics of Mb. Attempts were made to find a linear temperature dependence for the atomic displacements. Only 46 of the 153 amino acids in Mb show a temperature dependence that is consistant with

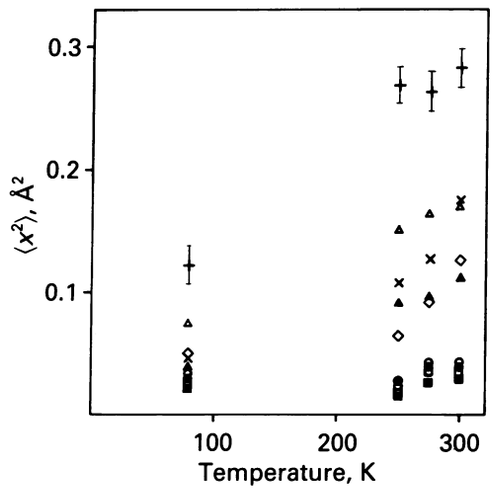

FIG. 2. Temperature dependence of $\langle x^2 \rangle$ values of some selected amino acids (backbone averages). +, glycine-121(GH3); ×, alanine-19(AB1); △, glutamic acid-83(EF6); ○, phenylalanine-138(H14); ●, leucine-11(A9); ■, valine-68(E9); □, alanine-71(E14); ▲, average of all nonhydrogen atoms; ◇, aspartic acid 126 (H2).

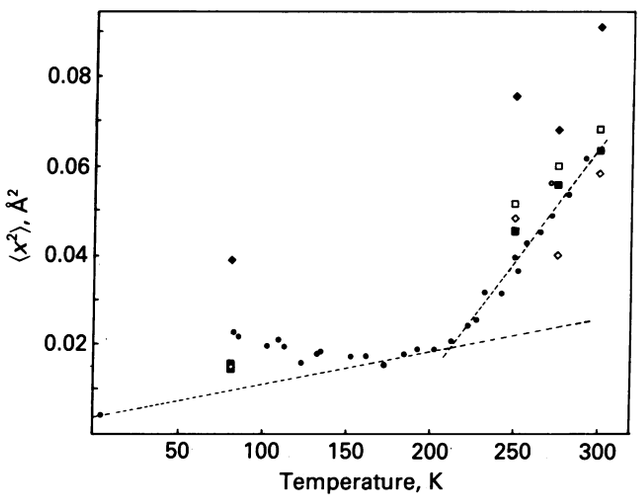

FIG. 3. Temperature dependence of $\langle x^2 \rangle$ values. ●, Fe measured by Mössbauer spectroscopy (13); ■, Fe determined by x-ray analysis; ◆, histidine-93(F8); ◇, histidine-64(E7).

a harmonic potential and relatively weak restoring forces, where the high-temperature portion of the $\langle x^2 \rangle$ vs. T curve extrapolates linearly to 0 at $T = 0$. An additional 51 amino acids can be modeled linearly vs. T with an average $\langle x^2 \rangle$ of 0.038 Å^2 at $T = 0$ (assuming an error limit of ± 0.015 Å^2). The large residual displacement at low temperature reflects the conformational substates of the molecule. The remaining 56 amino acids show no linear temperature dependence for the $\langle x^2 \rangle$ values of their backbone atoms, indicating anharmonic motion.

In Fig. 1, we see that Mb contains regions that have rather low $\langle x^2 \rangle$ values at 300 K. These $\langle x^2 \rangle$ values are nearly temperature independent. As examples, the $\langle x^2 \rangle$ values for leucine-11(A9), valine-66(E9), alanine-71(E14), and phenylalanine-138(H14) are given in Fig. 2. The temperature dependence and the absolute values of $\langle x^2 \rangle$ for these regions are close to those found for solids. In contrast alanine-19(AB1), glutamic acid-83(EF6), and glycine-121(GH3) display large $\langle x^2 \rangle$ values at 300 K and a strong temperature dependence. Thus, the protein has both "solid-like" and "semiliquid" regions.

Comparison with Mössbauer Data. Considering the many possible sources of error in the determination of $\langle x^2 \rangle$ by x-ray diffraction (10), it is gratifying that those for the iron atom obtained by crystallographic refinement at all four temperatures agree very well with the values obtained from Mössbauer absorption, where the errors are much smaller. The Mössbauer data in Fig. 3 show that the $\langle x^2 \rangle$ vs. T plot changes in slope around $T = 200$ K. Below 200 K, the temperature dependence of the iron atom $\langle x^2 \rangle$ is typical of that for atoms in solids. Above 200 K, the slope is much greater, indicating that new degrees of freedom of motion contribute. The small number of temperatures for which x-ray data are currently available do not permit a similar evaluation of the slope.

Heme Region. The average $\langle x^2 \rangle$ of the atoms of protoporphyrin IX is practically identical to the $\langle x^2 \rangle$ of the iron atom (Fig. 3). This behavior is confirmed by the electric hyperfine splitting of the Mössbauer spectrum, which senses the surroundings of the iron atom. If the atoms in the nearest coordination shell of the iron exhibited a different temperature dependence for their motions than that of the iron, there would be a discontinuity in the hyperfine splitting around 200 K. No discontinuity is observed (29).

At 80 K, just as at elevated temperatures (9), the distal side of the heme pocket is much more rigid than the proximal side. The temperature dependence of the residues is also different. For example, the distal histidine-64(E7) belongs to those amino acids for which $\langle x^2 \rangle \rightarrow 0$ as $T \rightarrow 0$. In contrast, the proximal histidine-93(F8) displays a much larger low-temperature $\langle x^2 \rangle$ (Fig. 3).

Conformational Substates at Low Temperatures. The observation of a nonexponential time dependence of the binding of CO and O_2 to Mb below 160 K was one reason for postulating conformational substates (7). A particular substate was assumed to give rise to an activation barrier of a given height; the distribution of substates consequently would yield a distribution of barrier heights that, in turn, would produce the nonexponential time dependence. Inspection of the mean-square displacements at 80 K near the iron atom and the heme group shows that $\langle x^2 \rangle$ is very small on the distal side. The largest displacements occur on the proximal side in the F helix, particularly in the residues on either side of the proximal histidine. This observation suggests that conformational substates of the F helix may control the motion of the iron into the heme plane on ligand binding; tension between histidine-93(F8) and Fe may be different in different substates.

Comparison with Theory. Three aspects of the data can be compared with molecular dynamics calculations: the individual $\langle x^2_i \rangle$ at 300 K, the temperature dependence of some selected $\langle x^2_i \rangle$, and the thermal contraction of the helices. M. Karplus and X. Swaminathan (private communication) have computed the mean-square displacements for Mb at 300 K and find, in general, reasonable agreement with the data (9). The temperature dependence of the $\langle x^2_i \rangle$ can be obtained by using a model anharmonic potential (29, 30) or by repeating the molecular dynamics calculations at various temperatures (31). The calculations and experiments show that detailed comparisons will yield essential information about the conformational motion in proteins.

Molecular dynamics calculations on isolated α-helices at 300 K and 80 K predict a dramatic reduction in the overall $\langle x^2 \rangle$ on cooling (31); subtracting our current best estimate, 0.025 Å^2, for the lattice disorder from our measured $\langle x^2_i \rangle$ values allows direct comparison of the two independent results. We observe average root-mean square displacements of 0.48 Å and 0.28 Å for the C_α atoms in the helices of myoglobin at 300 and 80 K, respectively. The corresponding values from molecular dynamics for the central C_α atoms in the isolated helix simulations are 0.52 Å at 300 K and 0.22 Å at 80 K (32). The agreement between the two methods gives confidence that both theory and x-ray experiments can give accurate information on the flexibility of proteins.

We thank Profs. W. Hoppe, M. Karplus, and R. L. Mössbauer for many useful discussions. We are grateful for financial support from the Bundesministerium für Forschung und Technologie (H.H. and F.P.), the National Science Foundation and the European Molecular Biology Organization (H.F.), and the National Institutes of Health (G.A.P., D.R.P., and H.F.).

1. Karplus, M. & McCammon, J. A. (1981) *CRC Crit. Rev. Biochem.* **99**, 293–349.
2. Gurd, F. R. N. & Rothgeb, T. M. (1979) *Adv. Protein Chem.* **33**, 74–156.
3. Cooper, A. (1980) *Sci. Prog. (Oxford)* **66**, 473–497.
4. Antonini, E. & Brunori, M. (1971) *Hemoglobin and Myoglobin in Their Reactions with Ligands* (North-Holland, Amsterdam).
5. Watson, H. C. (1969) *Prog. Stereochem.* **4**, 299–333.
6. Takano, T. (1977) *J. Mol. Biol.* **110**, 537–568.
7. Austin, R. H., Beeson, K. W., Eisenstein, L., Frauenfelder, H. & Gunsalus, I. C. (1975) *Biochemistry* **14**, 5355–5373.
8. Beece, D., Eisenstein, L., Frauenfelder, H., Good, D., Marden, M. C., Reinisch, L., Reynolds, A. H., Sorensen, L. B. & Yue, K. T. (1980) *Biochemistry* **19**, 5147–5157.
9. Frauenfelder, H., Petsko, G. A. & Tsernoglou, D. (1979) *Nature (London)* **280**, 558–563.
10. Frauenfelder, H. & Petsko, G. A. (1980) *Biophys. J.* **10**, 465–483.
11. Artymiuk, P. J., Blake, C. C. F., Grace, D. E. P., Oatley, S. J., Phillips, D. C. & Steinberg, M. J. E. (1979) *Nature (London)* **280**, 563–568.
12. Parak, F. (1980) *J. Phys. (Paris) Colloq. C1*, **41**, 71–78.
13. Parak, F., Frolov, E. N., Mössbauer, R. L. & Goldanski, V. I. (1981) *J. Mol. Biol.* **145**, 825–833.
14. Keller, H. & Debrunner, P. G. (1980) *Phys. Rev. Lett.* **45**, 68–71.
15. Eftink, M. R. & Ghiron, C. A. (1975) *Proc. Natl. Acad. Sci. USA* **72**, 3290–3294.
16. Krupyanskii, Yu., Parak, F., Engelman, D., Mössbauer, R. L., Goldanskii, V. I. & Suszcheliev, I. (1982) *Z. Naturforsch.* **37c**, 57–62.
17. Walter, J., Steigemann, W., Singh, T. P., Bartunik, H., Bode, W. & Huber, R. (1982) *Acta Crystallogr. Sect. B* **38**, 1462–1472.
18. Kendrew, J. C. & Parrish, R. G. (1957) *Proc. R. Soc. London Ser. A* **238**, 305–324.
19. Thomanek, U. F., Parak, F., Mössbauer, R. L., Formanek, H., Schwager, P. & Hoppe, W. (1973) *Acta Crystallogr. Sect. A* **29**, 263–265.
20. Douzou, P., Hui Bon Hoa, G. & Petsko, G. A. (1975) *J. Mol. Biol.* **96**, 367–380.
21. Parak, F., Mössbauer, R. L., Hoppe, W., Thomanek, U. F. & Bade, D. (1976) *J. de Phys. (Paris) Colloq. C6* **37**, 703–706.

22. Jones, A., Schwager, P. & Bartels, K. (1977) in *The Rotation Method in Crystallography*, eds. Arndt, U. W. & Wonacott, A. J. (North-Holland, Amsterdam), pp. 105–117.
23. Jones, T. A. (1978) *J. Appl. Crystallogr.* **11**, 268–272.
24. Konnert, J. H. & Hendrickson, W. A. (1980) *Acta Crystallogr. Sect. A* **36**, 344–349.
25. Mössbauer, R. L., Parak, F. & Hoppe, W. (1981) in *Mössbauer Spectroscopy II*, Topics in Current Physics, ed. Gonser, U. (Springer, Heidelberg), Vol. 25, pp. 5–30.
26. Richmond, T. J. & Richards, F. M. (1978) *J. Mol. Biol.* **119**, 537–555.
27. Parak, F. & Formanek, H. (1971) *Acta Crystallogr. Sect. A* **27**, 573–578.
28. Albertsson, J., Ockarsson, A., Stahl, K., Svensson, C. & Ymen, I. (1980) *Acta Crystallogr. Sect. B* **36**, 3072–3078.
29. Parak, F., Finck, P., Kucheida, D. & Mössbauer, R. L. (1981) *Hyperfine Interact.* **10**, 1075–1078.
30. Gavish, B. (1981) *Proc. Natl. Acad. Sci. USA* **78**, 6868–6872.
31. Mao, B., Pear, M. R. & McCammon, J. A. (1982) *Biopolymers*, in press.
32. Levy, R. M., Perahia, D. & Karplus, M. (1982) *Proc. Natl. Acad. Sci. USA* **79**, 1346–1350.